STATUS OF SwissFEL

F. Loehl for the SwissFEL team
Paul Scherrer Institut, Villigen PSI, Switzerland

Abstract

SwissFEL is a hard x-ray free-electron laser facility that is currently constructed at PSI. This paper gives an overview of the facility, describes the main sub-systems of the accelerator, and summarizes the installation and commissioning status.

INTRODUCTION

A schematic drawing of SwissFEL [1] is shown in Fig. 1. The accelerator is divided into an S-band injector, a C-band main linac (Linacs 1-3), and two undulator lines, Aramis and Athos. The Aramis line will provide hard x-ray radiation in the wavelength range from 0.1 – 0.7 nm and is part of the currently active first construction phase of SwissFEL. The soft x-ray undulator line Athos will cover the wavelength range from 0.6 – 4.9 nm and will be realized in a second phase from 2017 – 2020. The facility will operate at a repetition rate of 100 Hz.

The construction of the SwissFEL building started in spring 2013, and in summer 2015 the installation of first accelerator components begun. Today, October 2016, the vacuum line of the entire around 620 m long accelerator is close to being completed, and a first electron beam was generated and accelerated in the first 120 m of the facility.

INJECTOR

The electron source of the injector is an S-band gun [2] which was developed at PSI and first commissioned in the SwissFEL injector test facility [3]. This gun (for a picture see Fig. 2) combines design features of the LCLS gun and the CTF/PHIN gun. It has quadrupole-compensated symmetric couplers and is equipped with a load-lock system to allow for the exchange of cathodes. The gun is not equipped with tuning plungers and no tuning steps were applied during the manufacturing process. Instead, the gun is machined on frequency by using ultra-precision machining. While all the RF and mechanical design, as well as the brazing and most of the machining was performed at PSI, the ultra-precision machining took place at VDL-ETG. The nominal accelerating field at the cathode is 100 MV/m and the nominal energy gain is 7.1 MeV. As the cathode material, two options are available: copper or Cs_2Te. The baseline is Cs_2Te due to its higher quantum efficiency and its slower response time. The gun produced a first electron beam on August 24 of this year.

The electron beam from the gun is further accelerated in a total of six 4 m long S-band structures. The RF design of these structures was performed at PSI [4] and it includes dual-feed racetrack couplers and combines a constant gradient along the structure with a constant power loss. The structures were manufactured by Research Instruments. The first two structures are driven by an independent klystron, and the remaining four structures are grouped into two structures per klystron. After the first two structures, a laser heater is installed to circumvent the micro-bunch instability.

Two X-band structures follow the S-band section and are used to linearize the energy slope that the electron bunches obtain by being accelerated off-crest in the last four S-band structures. The X-band structures were designed and built in a collaboration between CERN, PSI, and Sincrotrone Trieste [5], and are followed by the first bunch compressor BC1 at a beam energy of 320 MeV. The injector ends with a diagnostics section that involves an S-band transverse deflecting structure that is used to setup the bunch compression.

C-BAND LINAC

The C-band Linac is divided into three segments: Linac 1, Linac 2, and Linac 3. After Linac 1, the electron bunches are further compressed in a second bunch compressor BC2 at an energy of 2.1 GeV. At the end of Linac 2, at 3.0 GeV of energy, a switch-yard [6] is installed with which electron bunches can be sent either straight into Linac 3 and consequently the hard x-ray Aramis line, or into the future soft x-ray line Athos. At the end of Linac 3, C-band transversely deflecting structures will be located that will allow for measurements of the longitudinal charge profile with a resolution of a few femtoseconds. These structures will arrive at PSI in February 2017 and are currently replaced by a vacuum pipe.

A total of 26 C-band modules are installed in the C-band Linac, and each module consists out of four C-band structures that are mounted onto two granite girders (see [7] for a schematic and [8] for further information). The C-band structures [9] are stacked and brazed at PSI [10] out of copper cells that were produced at VDL ETG (J-couplers) and VDL ETG Switzerland (regular cells) with micrometer precision using ultra-precision diamond milling and turning. This production process allows for avoiding any tuning steps while still achieving excellent field flatness and phase advance errors (for an example, see [7]). Furthermore, the achieved straightness of the structures is excellent: an example for a straightness measurement of a structure is shown in Fig. 3. The maximum measured deviations from a straight line are typically below 20 μm. In addition to the four structures, each Linac module also comprises a barrel open cavity (BOC) pulse compressor [11], and these were machined and brazed at PSI [12].

After the brazing, a vacuum leak test was performed for both the C-band structures and the BOC pulse compressors, and the RF properties were measured. Based on these RF measurements, a sorting of structures based on their resonance frequencies was performed with the goal of grouping four similar structures. This was necessary because all struc-

ISBN 978-3-95450-169-4

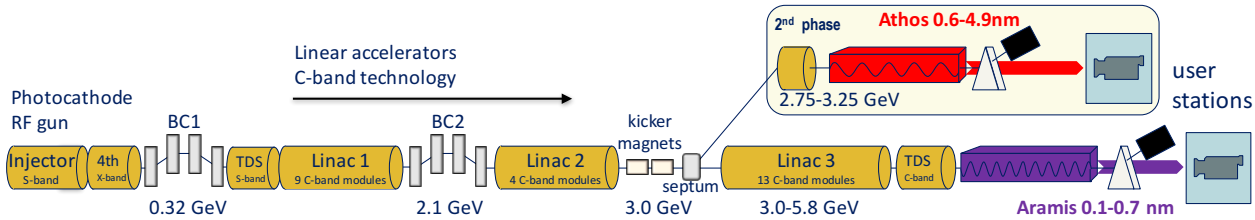

Figure 1: Schematic layout of the SwissFEL facility. It consists of an S-band injector, a C-band linear accelerator, and two undulator lines.

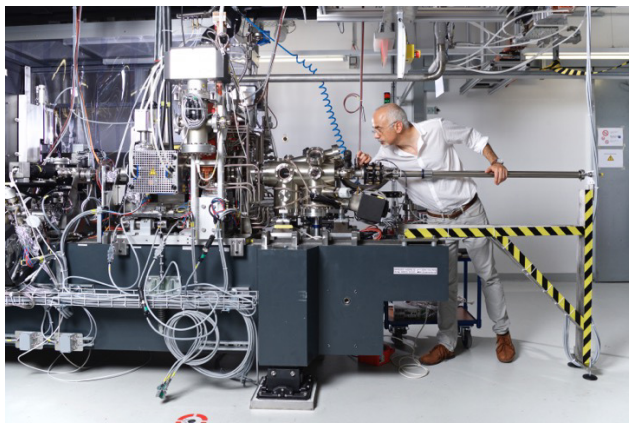

Figure 2: Picture of the gun area with the S-band gun and its load-lock system.

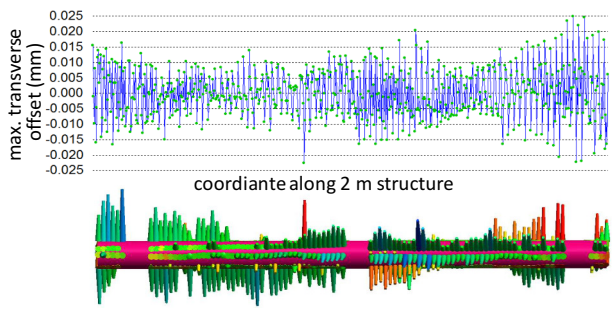

Figure 3: Example of a straightness measurement of a C-band structure (measurement by Tino Hoewler, PSI).

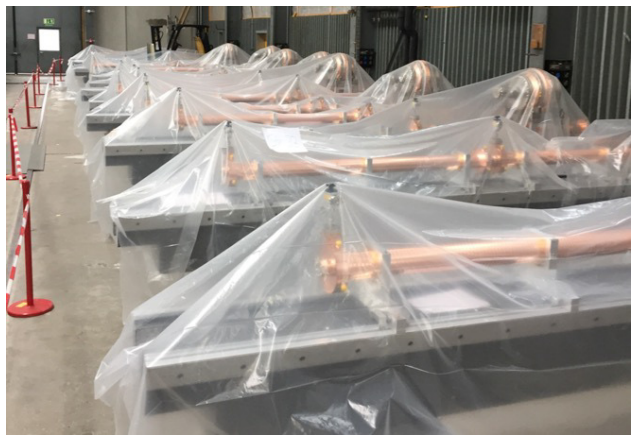

Figure 4: Storage area with pre-assembled C-band girders.

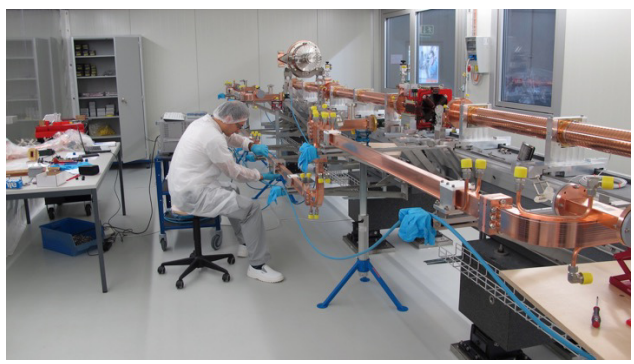

Figure 5: C-band module in the assembly hutch during the phase tuning of the waveguides.

tures of one module are cooled by a single cooling station. By this sorting, the additional RF power that is required to compensate for the loss in energy gain by not operating the structures at their resonance frequencies was limited to below 1% for almost all 26 modules.

The structures, pulse compressors, magnets, and beam diagnostics components were assembled onto the granite girders in a storage hall (see Fig. 4). From there, the girders were brought into an assembly hutch in which the waveguide network that was produced by MHI-MS was installed. One of the challenges of the waveguide network was the fact that four structures are supplied by RF power from a single RF source. The dimensions of the waveguides from structure to structure had to be accurate to within 200 μm to allow for a mechanical fit, and the phases at the entrance of the four structures also had to be correct within a few degrees. The first was ensured by MHI-MS during their manufacturing process by dimensional measurements of the individual waveguide components and accordingly machined correction pieces. To achieve the correct phase relations at the four structures, the complete horizontal waveguide network was assembled, moved away from the structures by using a rail system in order to allow for the installation of (shorting) flanges, and then the phase relations were measured using a network analyzer. The waveguides were then phase-tuned by proper deformations. As the last steps, the RF water loads delivered from CML were installed, the final vacuum connections between structures were made, and the modules were vacuum leak tested.

ISBN 978-3-95450-169-4

Figure 6: Installation of a C-band girder in the SwissFEL tunnel.

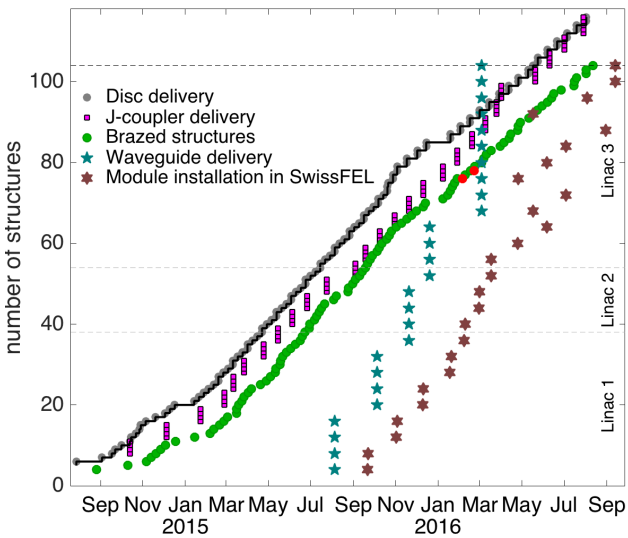

Figure 7: Delivery, production, and installation schedule for the C-band Linac.

The completed modules were then transported into the SwissFEL tunnel. Due to the fact that inside of the tunnel no crane is available, the transport and installation within the SwissFEL tunnel took place using custom-made transport tools (see Fig. 6). Once the girders were on their final locations, they were surveyed. Only an overall position adjustment of the girders was required because the alignment of individual components with respect to the alignment marks of the girders was already done during the girder assembly. The expected position accuracy of the individual pieces inside of the SwissFEL tunnel is on the order of 50 μm or below. As the last steps, the connecting waveguide pieces between girders were installed and the vacuum connections between the girders were made.

The manufacturing of the Linac modules followed a tight schedule that is depicted in Fig. 7. In about two years, all required accelerating structures were machined, and all Linac modules were assembled and installed in the SwissFEL tunnel. A picture of the Linac 1 area is shown in Fig. 8.

Figure 8: Picture of the Linac 1 area.

Figure 9: Hard x-ray undulator line of Aramis.

UNDULATORS

The Aramis line uses in-vacuum undulators with a period of 15 mm and a variable gap. Details about the undulators and the undulator line can be found in [13] and [14]. The mineral cast undulator frames were delivered into the SwissFEL building, where the installation of the magnet arrays, the magnet alignment and optimization, and the installation of the magnet arrays into the vacuum chamber took place. The 4 m long undulators with a weight of around 17 t were then transported to their final locations within SwissFEL using an air cushion vehicle. A picture of the undulator line is depicted in Fig. 9.

ISBN 978-3-95450-169-4

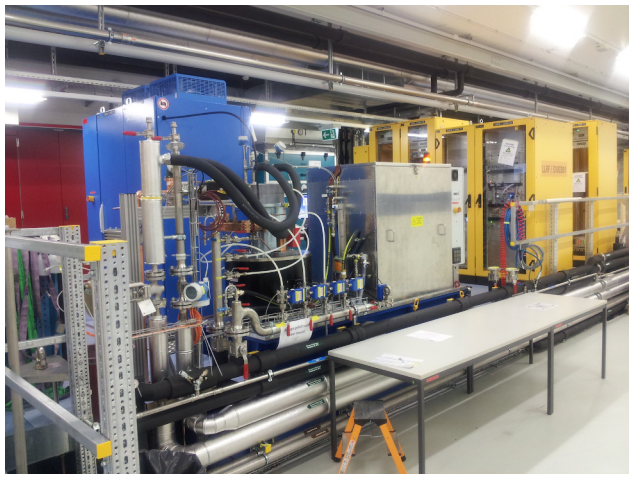

Figure 10: Picture of the RF power source of the first C-band module.

RF POWER SOURCES, RF CONDITIONING, AND FIRST BEAM OPERATION

All S-band stations use ScandiNova K2 solid-state modulators as the power source to drive Thales TH2100L klystrons. The modulators were moved from the 250 MeV SwissFEL injector test facility into SwissFEL and a number of upgrades and improvements have been done in that process. Besides the RF gun, the first two S-band stations are already conditioned, and a first electron beam with an energy of 150 MeV could be generated with these 3 RF stations and transported through the injector up to an intermediate beam dump in Linac 1 at a z-position of 120 m. The remaining two S-band stations are currently brought into operation and expected to be operational later this year. The X-band RF station that is driven by a SLAC XL5 klystron will follow these two stations.

The C-band Linacs 1 and 2 will be powered by Type-μ modulators from Ampegon, while Linac 3 will use PSI C-band series modulators M1071 from ScandiNova. The klystrons for the entire C-band linac are from Toshiba, type E37212, and all klystrons are already at PSI. PSI evaluated prototypes for both types of solid-state modulators and currently the companies are in the production process. The modulator installation in SwissFEL will start late this year and the installations, the commissioning, and subsequent RF conditioning will take place during the course of the next year with the goal of increasing the beam energy successively while modulators become available. SwissFEL is expected to reach its final beam energy of 5.8 GeV towards the end of next year.

To already test a first C-band module, the Ampegon Type-μ prototype modulator was installed at the first module of Linac 1 (see Fig. 10). The conditioning of the C-band module was mainly performed during nights to allow for installation work in the accelerator tunnel during working hours. Figure 11 shows the current progress. Almost the

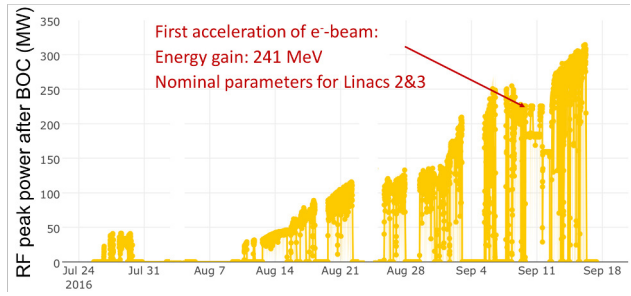

Figure 11: Conditioning progress for first C-band RF station.

maximum power from the klystron, 50 MW, was reached, yielding beyond 300 MW of power after the pulse compressor. During conditioning, only the last 100 ns of the up to 3 μs long flat-top of the RF pulse are compressed to yield high accelerating voltages but low energies in the breakdowns.

At an intermediate state during the conditioning, the power was reduced to 36 MW from the klystron, and the duration of the compressed pulse was set to the nominal 350 ns. This resulted in approx. 225 MW of peak power after the pulse compressor and corresponds to the nominal parameters of Linacs 2 and 3. With these settings, the energy gain of the electron beam was measured, yielding 241 MeV. Together with the energy from the S-band stations, a total energy of 391 MeV was reached. While there is still a small uncertainty in the measurements, this energy gain slightly exceeds the expectations and shows that the systems behave as designed.

OUTLOOK

In October 2016, the vacuum line of the entire accelerator will be closed and the goal is to establish transmission of the electron beam into the final beam dump after the Aramis undulator line by December 2016. During the course of 2017, the beam energy will then be further increased as RF stations become available, with the goal of reaching the final energy of 5.8 GeV at the end of the year. In summer 2017, first lasing of the FEL is expected, and first user experiments are planned for fall 2017.

REFERENCES

[1] R.Ganter (ed.), “SwissFEL Conceptual Design Report," PSI Bericht, 10-04, 2010.

[2] J.-Y. Raguin, M. Bopp, A. Citterio, A. Scherer, “The Swiss FEL RF Gun: RF Design and Thermal Analysis," in *Proc. of LINAC2012 Conf.*, Tel-Aviv, Israel, 2012, pp. 442–444.

[3] T. Schietinger *et al.*, “Commissioning experience and beam physics measurements at the SwissFEL Injector Test Facility," Phys. Rev. Accel. Beams, accepted September 1, 2016.

[4] J.-Y. Raguin, “The Swiss FEL S-Band Accelerating Structure: RF Design," in *Proc. of LINAC2012 Conf.*, Tel-Aviv, Israel, 2012, pp. 498–500.

ISBN 978-3-95450-169-4

[5] M. Dehler *et al.*, "Fabrication of the CERN/PSI/ST X-Band Accelerating Structures," in *Proc. of IPAC2011 Conf.*, San Sebastián, Spain, 2011, pp. 86–88.

[6] M. Paraliev, C. Gough, S. Dordevic, H. Braun, "High stability resonant kicker development for the SwissFEL switch yard," in *Proc. of 36th Int. Free-Electron Laser Conf.*, Basel, Switzerland, 2014, pp. 103–106.

[7] F. Loehl *et al.*, "Status of the SwissFEL C-band linear accelerator," in *Proc. 35th Int. Free-Electron Laser Conf.*, New York, USA, 2013, pp. 317–321.

[8] F. Loehl *et al.*, "Status of the SwissFEL C-band linear accelerator," in *Proc. of 36th Int. Free-Electron Laser Conf.*, Basel, Switzerland, 2014, pp. 322–326.

[9] J.-Y. Raguin and M. Bopp, "The SwissFEL C-band accelerating structure: RF design and thermal analysis," in *Proc. of the Linac 2012 Conf.*, Tel-Aviv, Israel, 2012, pp. 501–503.

[10] U. Ellenberger *et al.*, "Status of the manufacturing process for the SwissFEL C-band accelerating structures," in *Proc. of 35th Int. Free-Electron Laser Conf.*, New York, USA, 2013, pp. 245–249.

[11] R. Zennaro *et al.*, "C-band RF pulse compressor for SwissFEL," in *Proc. of the IPAC 2013 Conf.*, Shanghai, China., 2013, pp. 2827–2829.

[12] U. Ellenberger *et al.*, "The SwissFEL pulse compressor BOC: manufacturing and proof of precision by RF measurements," in *Proc. of 36th Int. Free-Electron Laser Conf.*, Basel, Switzerland, 2014, pp. 859–863.

[13] T. Schmidt *et al.*, "SwissFEL U15 Prototype Design and First Results in *Proc. 35th Int. Free-Electron Laser Conf.*, New York, USA, 2013, pp. 263–266.

[14] R. Ganter *et al.*, "Status of SwissFEL Undulator Lines," in *Proc. 34th Int. Free-Electron Laser Conf.*, Nara, Japan, 2012, pp. 666–669.